## Title

# Homogeneity and Isotropy of Compressed and Stabilized Earth Block Material: Mechanical Characterization and Statistical Analysis



## Journal

Journal of Materials in Civil Engineering, 36(10)

## ISSN

0899-1561

## Authors

Rengifo-López, Erika L
Kumar, Nitin
Matta, Fabio
et al.

## Publication Date

2024-10-01

## DOI

10.1061/jmcee7.mteng-17488

# Homogeneity and isotropy of compressed and stabilized earth block material: mechanical characterization and statistical analysis

**Erika L. Rengifo-López[1], Nitin Kumar[2], Fabio Matta[3]*, Michele Barbato[4]**

[1] PhD, Project Professional, GEI Consultants, Inc., 530 7th Avenue, Suite 2007, New York, NY 10018; formerly, Department of Civil and Environmental Engineering, University of South Carolina, Columbia, SC, USA; e-mail: erengifo@geiconsultants.com; ORCID iD: 0000-0002-2136-2639.

[2] PhD, Postdoctoral Scholar, S.M.ASCE, Department of Civil and Environmental Engineering, University of California, Davis, 3149 Ghausi Hall, Davis, CA, USA; e-mail: ntnkumar@ucdavis.edu. ORCID iD: 0000-0002-4045-300X.

[3] PhD, Associate Professor, M.ASCE, Department of Civil and Environmental Engineering, University of South Carolina, Columbia, 300 Main Street, Room C210, 29208 Columbia, SC, USA. * Corresponding author: tel +1 (803) 777-1917; e-mail: fmatta@sc.edu. ORCID iD: 0000-0001-7018-6611.

[4] PhD, Professor, F.ASCE, Department of Civil and Environmental Engineering, University of California, Davis, 3149 Ghausi Hall, Davis, CA, USA; e-mail: mbarbato@ucdavis.edu. ORCID iD: 0000-0003-0484-8191.

**ABSTRACT**

Compressed and stabilized earth block (CSEB) masonry is a locally appropriate alternative for low-rise dwellings that offer attractive affordability, sustainability, and durability features. From a designer's perspective, the availability of standards for material characterization and design codes is essential for CSEB masonry to be accepted and adopted. However, current standards and codes are limited—this is certainly the case in North America—and largely rely on empirical and prescriptive provisions that are adapted from those for conventional (*e.g.*, fired clay, cinder block) masonry. Advancing standardization and codification calls for advances in the fundamental understanding of material and structural behavior as a function of constituents and manufacturing methods. For CSEBs that are customarily compacted using metallic molds and hydraulic presses, a fundamental gap lies in the understanding of whether the heterogeneity of stabilized soil mixtures, together with the manufacturing process, result in block materials that can be approximated as homogeneous and isotropic at the scale of specimens used for physico-mechanical characterization. This paper reports on an investigation of a CSEB material whose constituent properties and manufacturing process are representative of those in North America. Homogeneity and isotropy are established based on empirical evidence from microscopic and chemical analysis, and on the statistical analysis of uniaxial compressive strength and stiffness data obtained from samples that were extracted from different areas of different source blocks, and tested by applying loads parallel or perpendicular to the compaction direction.

**Author keywords:** Earth block; Earth masonry; Homogeneity; Isotropy; Stabilized soil.

## INTRODUCTION

Compressed and stabilized earth blocks (CSEBs) are typically manufactured in a press using a soil mixture with a small amount of stabilizer such as cement and lime (Walker and Stace 1997, Vilane 2010). The use of CSEBs enables the construction of high-quality low-rise buildings that offer desirable sustainability features, such as affordability (*e.g.*, Kumar *et al.* 2018), durability (*e.g.*, Walker 2004), and lower embodied energy compared to fired clay and concrete masonry (Venkatarama Reddy and Jagadish 2003, Morton 2008). In addition, it is possible to engineer CSEB masonry structures that are capable of withstanding extreme loads due to natural hazards, including earthquakes (Morris *et al.* 2011) and high winds (Matta *et al.* 2015, Cuéllar-Azcárate 2016, Kumar *et al.* 2018, Erdogmus *et al.* 2019). In fact, earth masonry has been deployed in numerous applications in developed countries (*e.g.*, Germany, New Zealand, Switzerland), and may offer a locally-appropriate alternative to alleviate the growing shortage of affordable houses in North America. However, stabilized earth buildings remain uncommon and are typically perceived as substandard by owners. For example, in the US engineers may rely on a few standards (*e.g.*, ASTM 2016) and building codes based on empirical and prescriptive provisions (*e.g.*, NM CPR 2016, ICC 2021), which are typically adapted from fired clay and concrete masonry provisions.

Understanding the influence of constituents and manufacturing processes on the physical and mechanical properties of CSEB materials is necessary to underpin the development of standardized test methods as well as analysis and design tools. A fundamental knowledge gap exists on whether the intrinsic heterogeneity of stabilized soil mixtures enables the manufacturing of blocks whose materials can be regarded as homogeneous and isotropic at scales of ~10-100 mm, which are representative of specimens used for physico-mechanical characterization. The heterogeneity of stabilized soil mixtures accrues from the variety of particles having different sizes, shapes, morphologies, and chemical compositions (*e.g.*, Islam *et al.* 2020), and the amount and spatial distribution of water and stabilization compounds such as cement hydrates (Gooding 1994, González-López *et al.* 2018). The manufacturing process may also influence the degree of homogeneity and isotropy of CSEB materials, as reported for other masonry materials such as rammed earth (Bui and Morel 2009, Bui *et al.* 2009), extruded earth bricks (Aubert *et al.* 2016), and extruded fired clay bricks (Cabané *et al.* 2022). While mixing may be performed either manually or mechanically to obtain a similarly uniform mixture, quasi-static compaction may introduce inconsistencies even when using a hydraulic press. In particular, spatial variability of the dry density of CSEB materials may result from a non-uniform distribution of the compaction pressure, which depends on the compaction method (*e.g.*, single-sided, double-sided), magnitude of the pressure imparted, and friction between soil particles and, more importantly, between soil mixture and mold surfaces (Gooding 1993, 1994). In addition, quasi-static compaction of clayey soils may facilitate the formation of clusters of flaky clay particles that tend to be oriented perpendicularly to the compaction direction (Sloane and Kell 1966, Oliveira 2004). As a result, the preferential alignment of clay particles may constitute a significant source of anisotropy since the soils used for earth blocks have clay contents that are typically in the range 5-40% in weight (Jiménez Delgado and Cañas Guerrero 2007).

To the best of the author's knowledge, two studies offer some insight on the homogeneity and isotropy of CSEB materials. For a CSEB material incorporating 5% ordinary portland cement (OPC) in weight and compacted with a nominal pressure of 9.7 MPa, Gooding (1994) presented experimental evidence based on compression tests of cube specimens that were extracted from one single-sided compacted block, and one double-sided compacted block. Depending on the location where the specimens were extracted (*i.e.*, across the depth or the surface of the source CSEB), the compressive strength data differ on average by up to 15% and 4.5% for single-sided and double-sided compacted blocks, respectively. Gooding (1994) noted that a larger sample size is needed to understand whether the data variability is statistically significant, and validated these findings in relation to material homogeneity. González-López *et al.* (2018) reported compressive strength data for 30 mm × 40 mm × 200 mm CSEB-material specimens stabilized with 5% in weight of OPC or lime, compacted using different hydraulic presses, and tested by applying compressive forces either parallel or perpendicular to the direction of the compaction pressure. The results suggest that the CSEB material behaves less anisotropically as the compaction pressure and amount of stabilizer increase. No supporting information was provided on sample size and statistical analysis of test data.

This paper reports on an experimental and analytical investigation on the homogeneity and isotropy of a CSEB material made with a clayey soil that is common across the US, completing the research introduced in Rengifo-López *et al.* (2017, 2018). CSEB specimens were extracted from blocks that were manufactured through quasi-static hydraulic compaction. Microscopic inspection and elemental analysis were enlisted to characterize the micro-scale and meso-scale structure of the CSEB material. A statistically significant test matrix was designed including cube specimens that were load tested under uniaxial compression to characterize compressive strength and elastic stiffness. Homogeneity was investigated using specimens that were extracted at different locations (mid-block, corners) of the source CSEBs. Isotropy was investigated by applying the compressive load either parallel or perpendicular to the direction of the compaction pressure. A statistical analysis was performed to understand the statistical significance of the differences between strength and stiffness data as a function of cube specimen location, and compressive load direction vis-à-vis compaction direction.

## SIGNIFICANCE

Similar to other cementitious composites (*e.g.*, mortar, concrete), the uniaxial compressive strength is the main property used to characterize the durability and mechanical performance of CSEB materials. Current material characterization and structural analysis practices rely on the assumption that CSEB materials are homogeneous and isotropic with respect to compressive strength. For example, this is a typical assumption for numerical models (*e.g.*, Miccoli *et al.* 2015, Kumar *et al.* 2022, 2023) as well as compression strength characterization since uniaxial loads are customarily imparted in the direction parallel to that of compaction (*e.g.*, Walker and Stace 1997, Walker 2004, Piattoni *et al.* 2011, Matta *et al.* 2015, Cuéllar-Azcárate 2016, Islam *et al.* 2020). Therefore, establishing if and at what scale representative CSEB materials may be approximated as homogeneous and isotropic has practical implications for manufacturing, standardization, structural analysis and numerical modeling, and ultimately design.

## EXPERIMENTAL PROGRAM

### Materials

#### *Soil*

The soil used in this research was sourced from a pit in Lexington, SC [**Fig. 1(a)**]. The soil was air dried, crushed in a mechanical mixer using 12 steel balls with a 48-mm diameter, and sieved using a standard No. 8 mesh (nominal opening = 2.36 mm) as reported in Rengifo-López (2022). The resulting soil is shown in **Fig. 1(b)**. **Fig. 1(c)** presents the soil gradation curve as determined according with ASTM D6913 (ASTM 2017d) and ASTM D7928 (ASTM 2017c). For a given sieve size, the data indicate the average and standard deviation (SD) of the percent passing based on measurements on five soil samples with an average mass of 540 g (SD = 42.5 g).

The Atterberg limits and optimum moisture content were characterized in accordance with ASTM D4318 (ASTM 2017b) using six soil samples and ASTM D698 (ASTM 2012) using four soil samples, respectively. **Table 1** presents the resulting average and SD values for sand, silt and clay content, liquid limit, plastic limit, plasticity index, and optimum moisture content. Based on the criteria specified in ASTM D2487 (ASTM 2017a), the soil was classified as a clayey sand (SC). As a result, the soil selected for this investigation is characterized by composition and properties that are representative of typical soils that are suitable for earthen construction (*e.g.*, Jiménez Delgado and Cañas Guerrero 2007, Morton 2008).

***Compressed and stabilized earth blocks***

The soil in **Fig. 1** was used to manufacture CSEBs with nominal dimensions of 254 mm × 178 mm × 89 mm following the procedure detailed in Cuéllar-Azcárate (2016). A soil mixture containing Type I OPC (6% in weight) and water (20% in weight) was used. The higher amount of water compared to the Proctor test-based optimum moisture content in **Table 1** was selected based on evidence from ball drop tests (Rigassi 1985, Islam *et al.* 2020). The choice of OPC as stabilizer reflects a realistic intent to facilitate the initial acceptance of a technology, which is not mainstream yet, by using a material that is suitable to enhance strength and durability, widely available, and familiar to builders. In this instance, it is noted that the amount of OPC is sufficient to yield a two-fold increase in compressive strength compared to counterpart unstabilized earth blocks (Matta et al. 2015) while lying well below typical weight ratios of OPC to fine and coarse aggregates (~10%). However, the overarching perspective is also to demonstrate proof-of-concept and contribute to paving the way for other sensible and environmentally sustainable stabilization strategies (Van Damme and Houben 2018), rather than solely pursuing the development of another form of low-strength OPC-based composite.

The mixture was placed into a steel mold and then compressed at a nominal pressure of 10 MPa using a commercial hydraulic press (model EPH-2008, Fernco Metal Products, Capitan, NM), as illustrated in **Fig. 2(a)**. The CSEBs were cured indoors for 14 days while tightly wrapped in plastic sheets. Upon removal of the plastic sheets, the CSEBs were air cured indoors for a minimum of 90 days prior to extracting the specimens for the material microstructural, chemical, and mechanical characterization.

Upon curing, the average density of 1701 kg/m$^3$ (SD = 66.6 kg/m$^3$) was determined based on the measured mass and side lengths of seven specimens having 127 mm × 127 mm × 89 mm nominal dimensions, which were cut from four CSEBs using a diamond saw blade. Then, these specimens were crushed using a loading frame to extract smaller samples, which were weighted and then oven-dried at a temperature of 110°C for 24 hours. These samples were used to characterize the average moisture content of 2.38% (SD = 0.45%) and average dry density of 1660 kg/m$^3$ (SD = 63.5 kg/m$^3$). Coherently with the stated research significance, it is emphasized that the manufacturing procedure was intended to yield CSEB specimens whose density and moisture content are representative of in-service conditions (*e.g.*, González-López et al. 2018) rather than to be used for quality control purposes. In the latter case, characterizing the strength of wet specimens after pre-soaking may be preferable (*e.g.*, Walker 2004).

## Microstructural and chemical characterization

Scanning electron microscopy (SEM) analysis was enlisted to visually examine the microstructure of the CSEB material at the micro- and meso-scale. In combination with SEM analysis, energy dispersive spectroscopy (EDS) analysis was used for the chemical (elemental) characterization. The tests were performed using a variable-pressure scanning electron microscope with integrated EDS capabilities (model VEGA3 SBU, TESCAN, Czech Republic) on a total of 16 sample surfaces, each with an area of 5 mm × 5 mm, which were randomly selected from four 10 mm × 10 mm × 10 mm cubic samples that were cut from mid-block and corner portions of source CSEBs. Each sample was mounted on aluminum stubs using adhesive carbon tabs, and then coated twice using a gold target (model Desk II, Denton Vacuum, Moorestown, NJ). Testing yielded 120 SEM micrographs with magnification ranging from ~50× to ~25,000× and 42 EDS elemental maps.

## Mechanical characterization

### *Test matrix*

Uniaxial compression tests were performed on a total of 84 76-mm cube specimens that were wet-cut from 14 CSEBs using a diamond saw blade and dried in an indoor laboratory environment for one week. Each cut surface was inspected to assess its dryness, integrity, and the absence of visible cracks. As illustrated in **Fig. 2(b)**, six cube specimens were obtained from each CSEB, including four "corner" specimens (denoted as C1 through C4), each having two lateral surfaces in contact with the steel mold during manufacturing, and two "mid-block" specimens (denoted as M1 and M2). **Table 2** summarizes the test matrix, which was designed to produce a suitable dataset to assess:

- homogeneity, based on the uniaxial strength and elastic stiffness of specimens cut from different locations, *i.e.*, "C" for corners, and "M" for mid-block; and,
- isotropy, based on the uniaxial strength and elastic stiffness of specimens loaded in different orthogonal directions, *i.e.*, "X" and "Y" perpendicular and "Z" parallel to the compaction direction during manufacturing, respectively.

In fact, each group of four "C" cubes and two "M" cubes extracted from a given CSEB includes specimens that are nominally identical since they were subjected to: (i) a similar pressure during compaction; (ii) similar boundary conditions during compaction; and (iii) a similar cutting process. From each CSEB, two randomly selected cube specimens were tested for each loading direction, for a total of 28 specimens for X, Y, and Z, respectively, including 56 corner specimens and 28 mid-block specimens. This approach aimed to minimize the number of CSEBs needed to obtain a sufficient number of cube specimens to derive strength and stiffness statistics for each loading direction.

***Uniaxial compression test setup and procedure***

The test setup is illustrated in **Fig. 3**. Each cube specimen was centered between two 51-mm thick steel platens. A 0.4-mm thick polytetrafluoroethylene (PTFE) insert was placed between the specimen and each platen to minimize constraining effects due to friction. For the case of adobe, these effects have been documented by Illampas *et al.* (2014). The uniaxial compressive load was applied monotonically up to failure, at a displacement rate of 0.03 mm/s, using a servo-controlled hydraulic test frame with a capacity of 245 kN. The load was measured using a 45-kN load cell sandwiched between the top platen and the loading apparatus. Vertical displacements were measured using four linear transducers that were rigidly mounted onto the bottom platen.

## RESULTS AND DISCUSSION

First, the empirical (SEM and EDS) evidence on the microstructure and chemical composition of the CSEB material at the micro- and meso-scale is presented and discussed, highlighting the qualitative and quantitative findings that relate to homogeneity and isotropy. Second, the results of the compression tests are used to generate datasets for two key mechanical parameters, namely, compressive strength and elastic stiffness. These datasets serve as a quantitative means to: (i) assess homogeneity and isotropy based on CSEB specimen location and loading direction, respectively; and (ii) highlight the need of statistical analysis to rigorously draw conclusions.

### Visual and chemical characterization

#### *Microstructure*

Representative SEM micrographs of the CSEB material at increasing magnifications (~50× to ~10,000×) are shown in **Fig. 4**. At the meso-scale, which is depicted in **Fig. 4(a)**, coarser (sand) particles with size in the range ~0.1-1 mm are distributed throughout and embedded in a compacted matrix of stabilized soil with finer particles. The interface discontinuities between coarser particles and surrounding matrix are illustrated in the close-up image of a sand grain in **Fig. 4(b)**; this image highlights the importance of using soil mixtures having a limited and well-distributed volume of sand in a stabilized soil matrix to hinder the formation of interphases and weaker areas. The typical pore size and distribution are more visible at the micro-scale, as shown in **Fig. 4(c)** where pores with size of ~10 μm or less are relatively well distributed through the soil matrix. Further increasing the magnification enables one to appreciate the micro-scale heterogeneity of the CSEB material; for example, in **Fig. 4(d)** the characteristic flaky shape of clay particles with different sizes and orientations can be observed.

The evidence obtained through SEM analysis illustrates: (i) the relatively low porosity that accrues from compaction and stabilization, and whose consistency in the pore size and spatial distribution may not affect homogeneity more adversely than the morphology and distribution of the solid particles and phases; and (ii) how the CSEB material heterogeneity, which is evident at the micro-scale, fades at decreasing magnifications, and thus at scales that are relevant for the characterization of mechanical properties suitable for structural analysis and design.

***Chemical composition***

The main chemical elements were identified through quantitative EDS analysis of salient spectra vis-à-vis default data available for all chemical elements through the equipment used (Newbury and Ritchie 2013). **Fig. 5** presents the mass concentrations in seven randomly selected CSEB sample areas at magnifications ranging from ~100× to ~5000×. It is noted that oxygen (O), aluminum (Al), and silicon (Si) provide the main peaks in the EDS spectra of kaolinite, a common clay mineral whose presence is expected in the soil used in this research. All elements, including carbon (C), O, Al, Si, potassium (K), iron (Fe), and calcium (Ca), are consistently well distributed irrespective of range of concentration (*i.e.*, mass %) and image magnification (**Fig. 5**), thus indicating that the CSEB material has a fairly homogeneous chemical composition.

Since Ca was not detected in the unstabilized soil—as also reported by Cuéllar-Azcárate (2016) for soil sourced from the same location—the two-dimensional EDS mapping capabilities of the integrated SEM/EDS instrument were enlisted to assess the presence and distribution of Ca as an indicator of the cement hydrates resulting from soil stabilization. **Fig. 6** presents the Ca maps for three CSEB sample areas, which were selected among the seven that yielded the results in **Fig. 5** to provide representative results within a comparable range of magnifications (~100× to ~5000×). It is noted that Ca was not detected in areas where sand particles or large voids are located; otherwise, cement hydrates are similarly well distributed throughout the stabilized soil matrix from the meso-scale [**Fig. 6(a-b)**] to the micro-scale [**Fig. 6(b-c)**].

## Mechanical characterization

All CSEB cube specimens subject to uniaxial compressive loads failed in a quasi-brittle fashion. As shown in **Fig. 7** for specimens loaded in different directions, columnar (vertical) cracks developed since the early stages of testing [*e.g.*, **Fig. 7(a)**], indicating that the test setup (**Fig. 3**) was effective in mitigating frictional effects. The compressive load (and stress)-displacement response envelopes, together with the curves for 15 representative specimens, are presented in **Fig. 8** as a function of specimen location (C, M in **Fig. 2**), and in **Fig. 9** as a function of load direction (X, Y, Z in **Fig. 2**).

### *Compressive strength*

**Table 3** reports the compressive strength, $f_{CSEB}$, for all specimens, together with the mean and coefficient of variation (CV) for each group of six specimens extracted from each one of the 14 CSEBs (B01 through B14). For a given source CSEB, the mean $f_{CSEB}$ and CV were in the range

1.64-4.70 MPa and 8.9-21.2%, respectively. It is noted that the ranges of CV obtained in this study are consistent with data reported in the literature for earth block materials (*e.g.*, Ciancio and Gibbings 2012, Silveira *et al.* 2013, Ruiz *et al.* 2018). To discuss these results vis-à-vis material homogeneity and isotropy, **Table 4** summarizes the mean $f_{CSEB}$ and the CV for six groups of specimens, namely "All", "C" and "M" (grouped by location), and "X", "Y" and "Z" (grouped by load direction). For the entire dataset, the mean and CV are 3.40 MPa and 29.3%, where the former is suitable for structural applications (*e.g.*, Matta *et al.* 2015).

When assessing the results based on location, it is noted that mid-block (M) specimens have an average strength that is 6.3% greater and less variable than corner (C) specimens. This result may not be explained by the cutting process since the M and C specimens were manufactured by wet-cutting on four and three surfaces, respectively. Instead, this result may be influenced by frictional effects at the soil-mold interface resulting in areas of less effectively compacted material compared to the mid-block region. However, given the limited differences in both strength and variability, statistical analysis is needed to understand whether these differences are significant enough to conclude that the CSEB material is not homogeneous at the scale of the cube specimens used in this research.

When assessing the results based on load direction, it is noted that the specimens loaded in the compaction direction (Z) have an average strength that is 11.5% and 9.2% smaller and more variable than those loaded in the orthogonal directions X and Y, respectively. This empirical evidence suggests that the CSEB material is not necessarily characterized by a greater strength in the direction parallel to that of quasi-static compaction. However, given the limited differences in both strength and variability, statistical analysis is needed to understand whether these differences are significant enough to conclude that the CSEB material is not isotropic at the scale of the cube specimens used in this research.

***Elastic stiffness***

Based on the axial load-displacement data summarized in **Fig. 8** and **Fig. 9**, the elastic stiffness was calculated as the slope of the linear portion of a given curve at a stress equal to $0.5f_{CSEB}$. **Table 5** reports the elastic stiffness, $K_{CSEB}$, for all specimens, together with the mean and CV for each group of six specimens (five in one instance where displacement measurements were not acquired) extracted from each CSEB. For a given source CSEB, the mean $K_{CSEB}$ and the CV were in the range 9.10-18.6 kN/mm and 10.1-22.7%, respectively. **Table 6** summarizes the mean $K_{CSEB}$ and the CV for six groups of specimens, similar to **Table 4**. For the entire dataset, the mean and CV are 13.3 kN/mm and 36.6%, thus consistent with the variability observed for $f_{CSEB}$. It is noted that the variability of both unconfined compressive strength and elastic stiffness is an order of magnitude greater than that of the average density of the CSEB material (CV = 3.9%), indicating that the latter may not be sufficient to explain the former.

The results based on specimen location and load direction are consistent with the strength results in **Table 4**. The mid-block (M) specimens have an average stiffness that is 3.81% greater than the corner (C) specimens, which may support the conclusion that the CSEB material is homogeneous. However, the specimens loaded in the compaction direction (Z) have an average stiffness that is 16.0% and 9.7% smaller and more variable than those loaded in the orthogonal directions X and Y, respectively. This empirical evidence suggests that the elastic stiffness may depend on the compaction direction. The significance of these differences is investigated based on statistical analysis, as reported in the next section.

## STATISTICAL ANALYSIS

To quantitatively support conclusions on the homogeneity and isotropy of the CSEB material based on the datasets provided in **Table 3** through **Table 6**, statistical analysis was enlisted to study the influence of specimen location and load direction on compressive strength and elastic stiffness. First, the dispersion of the experimental data was graphically analyzed using notched box plots (NBPs). Second, analysis of variance (ANOVA) and Levine's test were employed to investigate the statistical difference between the mean values and variances of $f_{CSEB}$ and $K_{CSEB}$ for specimens groups based on location (C, M) and load direction (X, Y, Z). Third, confidence intervals of the mean and SD estimators were calculated and then used to assess the appropriateness of the experimental sample sizes. Fourth, a goodness-of-fit test was performed to identify appropriate statistical distributions for the experimental data.

### Visualization of data dispersion through notched box plots

The notched box plots (NBPs) in **Fig. 10** and **Fig. 11** present the experimentally determined values of $f_{CSEB}$ and $K_{CSEB}$, respectively, for the six CSEB specimen groups in **Table 4** and **Table 6**. Notched box plots are effective in graphically describing the statistical variability of datasets. In an NBP, the central mark indicates the median; the lower and upper hinges of the box enclose the interquartile range (IQR), *i.e.*, identify the dataset's $25^{th}$ and $75^{th}$ percentiles, respectively. A given notch indicates the 95% confidence interval of the median value, which may be used as an indicator of the statistical difference between medians of different datasets (McGill *et al.* 1978).

The upper and lower values are linked to the hinges through dashed lines ('whiskers'), and the difference between these values is referred to as 'range'. The spacing between the different parts of the box for a given group *(i.e.,* the median, upper hinge, lower hinge, and whiskers) graphically describes the degree of data dispersion and skewness.

In **Fig. 10**, the range of $f_{CSEB}$ (*i.e.*, the difference between upper and lower value) for the six different groups is between 3.6 MPa and 4.2 MPa, the IQR lies in the range 1.23–1.96 MPa, and the CV varies between 26.1% and 32.8%, indicating that the datasets for all groups exhibit a significant variability. It is noted that the data are approximately symmetrically distributed about the median for all groups except for the specimens loaded in the compaction (Z) direction. The notches present a significant albeit partial overlap for the specimens grouped by location. A similar observation applies to groups X and Y; instead, the notches of groups X and Z and of groups Y and Z present a relatively small overlap. To identify any statistically significant differences between the medians of the different groups, a Wilconox rank-sum test (Hollander *et al.* 2015) with a significance level equal to 0.05 was performed. As reported in **Table 7**, the resulting $p$-values $\geq$ 0.12 consistently indicate that the difference between the medians of different groups are not statistically significant.

In **Fig. 11**, the range of $K_{CSEB}$ for the six different groups is between 15.8 and 17.4 kN/mm, the IQR lies in the range 6.1–9.8 kN/mm, and the CV varies between 33.7% - 38.6%, indicating that also these datasets for all groups exhibit a significant variability. Similar to the $f_{CSEB}$ data other than group Z, the $K_{CSEB}$ data for all groups are approximately symmetrically distributed about their medians. In addition, all groups present significant overlaps between the confidence intervals of their medians. As reported in **Table 8**, the resulting *p*-values ≥ 0.12 consistently indicate that the difference between medians of different groups are not statistically significant.

**Assessment of mean values for $f_{CSEB}$ and $K_{CSEB}$ through ANOVA**

One-way ANOVA was enlisted to assess statistical differences among mean values of $f_{CSEB}$ and $K_{CSEB}$ by comparing the sample variation among different specimen groups with the sample variation within each group (Rutherford 2011). The statistical test used herein is based on the following three assumptions (Lix *et al.* 1996; Rutherford 2011): (1) independence of observations, (2) homogeneity of data variances, and (3) normal distribution of residuals. The first assumption is satisfied because the specimens from any given block were randomly grouped by location and load direction to assemble the text matrix summarized in **Table 2**. In addition, whereas each CSEB material specimen is representative of a specific location and load direction as illustrated in **Fig. 2**, the effect of each variable was analyzed independently. The verification of the second and third assumptions is presented in the remainder of this paper. It is noted that the results from ANOVA exhibit weak sensitivity to departures from normality (Glass *et al.* 1972; Lix *et al.* 1996); however, the effects of violating the assumption of homogeneity of data variance can be significant when group sizes are not equal (Lix *et al.* 1996), as it is the case of the specimens grouped by location, for which group M and group C include 28 and 56 specimens, respectively.

The resulting *p*-values for $f_{CSEB}$ from ANOVA are 0.49 and 0.28 for specimens grouped by location (C, M) and by load direction (X, Y, Z), respectively. The resulting *p*-values for $K_{CSEB}$ are 0.91 and 0.23 for specimens grouped by location and by load direction, respectively. All *p*-

values exceed the significance level of 0.05, which indicates that neither the mean $f_{CSEB}$ nor the mean $K_{CSEB}$ differ among the groups in a statistically significant manner. These results do not support the null hypothesis that the different specimen groups considered in this study share different mean values of compressive strength and elastic stiffness.

**Verification of assumption of homogeneity of data variances**

Levene's test was enlisted to verify the homogeneity of data variances among different groups. This test was selected because of its simplicity and insensitivity to the violation of the normality assumption (Levene 1960, Glass 1966). The assumption of homogeneity of data variances is satisfied when the error variance across all predicted values of a dependent variable is constant (Rutherford 2011). In this case, Levene's test was used to verify if the population variances for the different groups exhibit statistically significant differences by assuming a significance level equal to 0.05.

The resulting *p*-values from Levene's test on the $f_{CSEB}$ data are 0.49 and 0.28 for specimens grouped by location (C, M) and by load direction (X, Y, Z), respectively. The resulting *p*-values from Levene's test on $K_{CSEB}$ data are 0.91 and 0.23 for specimens grouped by location and by load direction, respectively. For both mechanical parameters, the *p*-values are greater than the significance level of 0.05, indicating that the differences among the data variances of these specimen groups are not statistically significant. Therefore, the results of Levene's test indicate that all specimen groups share similar variance values for both compressive strength and elastic stiffness, thereby corroborating the assumption of homogeneity of data variances for ANOVA.

The combined results of ANOVA and Levine's test suggest that all data groups belong to the same population, and that a single probability distribution may be used to describe the variability of all results. Therefore, these results support the conclusion that compressive strength and elastic stiffness are homogeneous and isotropic properties for the representative CSEB material.

**Assessment of accuracy of mean and standard deviation estimation**

The accuracy of the mean and SD estimators of $f_{\mathrm{CSEB}}$ and $K_{\mathrm{CSEB}}$ for the different specimen groups was investigated by means of confidence intervals, and coefficient of variation (CV), of the mean and SD estimators. Confidence intervals provide a graphical representation of the estimated range of variation for each of the unknown population parameters (*i.e.*, mean and SD). In particular, the 95% confidence intervals used hereinafter indicate the range within which each parameter estimator is expected to be found 95% of the times that the experiment is performed (Streiner 1996, Harding *et al.* 2014). Confidence intervals and standard errors of means and SD were calculated according to the approximate equations given in Harding *et al.* (2014). These equations are valid for sample sizes larger than or equal to 10 for the mean and 20 for the standard deviation. All specimen groups satisfy these conditions.

For all groups, the confidence intervals for the estimators of the mean and SD of compressive strength and elastic stiffness are presented in **Fig. 12** and **Fig. 13**, respectively. The CVs of the mean and SD estimators of compressive strength and elastic stiffness are reported in **Table 9** and **Table 10**, respectively. The 95% confidence intervals of the mean and SD estimators for the specimens grouped by location (C, M) and load direction (X, Y, Z) present a significant partial overlap with each other for both mechanical parameters.

The $p$-values obtained from a two-sample $t$-test (Snedecor and Cochran 1989) for the means of $f_{CSEB}$ and $K_{CSEB}$ are reported in **Table 11** and **Table 12**, respectively. These results indicate that, assuming a significance level equal to 0.05, the differences between the means of any couple of specimen groups are not statistically significant, since $p$-values $\geq 0.15$ for the means of $f_{CSEB}$, and $p$-values $\geq 0.10$ for the means of $K_{CSEB}$. Similarly, the $p$-values obtained from a two-sample $F$-test for the SDs of $f_{CSEB}$ and $K_{CSEB}$ are reported in **Table 13** and **Table 14**, respectively. These results indicate that, assuming a significance level equal to 0.05, the differences between the SDs of any couple of specimen groups are not statistically significant, since $p$-values $\geq 0.44$ for the SDs of $f_{CSEB}$, and $p$-values $\geq 0.42$ for the SDs of $K_{CSEB}$. The CVs of the mean estimator for different sample groups attain values between 3.2% and 5.6% for $f_{CSEB}$, and between 4.0% and 7.3% for $K_{CSEB}$. The CVs of the SD estimator of different sample groups assume values between 7.7% and 13.7% for $f_{CSEB}$, and between 7.8% and 13.6% for $K_{CSEB}$. Customarily, a CV $\leq$ 14% is considered acceptable for the estimation of a statistical parameter, for example as in the FEMA 356 recommendations on sample sizes for concrete compressive strength (ASCE 2000, *Sec. 6.3.2.4.1*). Therefore, it is concluded that the mean and SD estimates obtained in this study are sufficiently accurate (*i.e.*, the CVs are sufficiently small) for both $f_{CSEB}$ and $K_{CSEB}$ for all specimen groups.

**Assessment of statistical distribution of experimental data**

Once it was established that the CSEB material can be regarded as homogeneous and isotropic with respect to compressive strength and elastic stiffness, a goodness-of-fit technique was used to identify suitable probability distributions for these two mechanical parameters (Montgomery *et al.* 2009, Gibbons and Chakraborti 2020). Establishing suitable probability distributions for salient mechanical properties is of practical significance, such as for applications concerning structural reliability, probabilistic structural response, structural dynamics, uncertainty quantification, risk management, and probabilistic life-cycle cost analysis.

The Anderson-Darling (AD) test for continuous distributions with unknown parameters, in which both location (mean) and scale (variance) are estimated from the samples (D'Agostino and Stephens 1986; Kececioglu 2002), was used. The probability distributions considered in the test are normal, log-normal, and truncated normal (with a lower truncation for values smaller than zero). The AD test was selected because it is one of the most effective statistical tools for detecting departures from normality (Stephens 1974, 1986), and attributes more weight to the distribution tails than other equivalent tests such as the Kolmogorov-Smirnov test (Stephens 1974). The AD test was performed on the data for all CSEB specimens (group "All" including 84 data for $f_{CSEB}$, and 83 data for $K_{CSEB}$). A significance level of 0.05 was selected to determine whether a given distribution is acceptable. The maximum difference between the empirical cumulative distribution function (CDF) and the analytical CDF was compared with the critical value corresponding to the desired significance level (Kececioglu 2002).

For each statistical distribution, the calculated *p*-values are presented in **Table 15**. It is noted that the *p*-values for the log-normal distribution of both compressive strength and elastic stiffness are less than 0.05; thus, the hypothesis of log-normal distribution can be rejected for the selected significance level. Instead, the calculated *p*-values for the normal distribution and truncated normal distribution are similar and greater than 0.05 for both compressive strength and elastic stiffness; thus, for practical purposes, these statistical distributions are similarly suitable to describe the variability of $f_{CSEB}$ and $K_{CSEB}$ for the representative CSEB material from one-side-compressed blocks. However, it is noted that the *p*-values for the normal distribution are slightly greater than those for the truncated normal distribution. In addition, the use of a normal distribution is typically simpler and more computationally efficient than the use of a truncated normal distribution, although the former could produce physically unrealizable negative values in applications requiring stochastic sample generation. Therefore, the normal distribution appears to be most suitable for applications focused on the body of the distribution (*e.g.*, probabilistic response, stochastic dynamics), whereas the truncated normal distribution appears to be most suitable for applications focused on the distribution tails (*e.g.*, structural reliability).

## CONCLUSIONS

The CSEB material discussed in this paper is representative of typical earth block materials that are suitable for masonry construction in North America, based on soil composition and properties, type and amount of stabilizing agent, and manufacturing process. Based on the results of the experimental characterization and statistical analysis presented herein, the following conclusions are drawn.

1) Based on evidence from SEM analysis, physical heterogeneity is evident at the micro-scale and fades past the meso-scale, supporting the hypothesis that the CSEB material is homogeneous at a scale that is representative of specimens used to characterize compressive strength for structural analysis and design purposes.
2) Evidence from EDS analysis indicates that the main chemical elements are well distributed throughout the stabilized soil matrix irrespective of the range of concentration and image

magnification. In particular, the spatial distribution of Ca at the micro-scale and meso-scale indicates that the cement hydrates resulting from stabilization are uniformly distributed, thereby contributing to the CSEB material homogeneity, consistent with the findings of the SEM analysis.

3) The uniaxial compressive strength and elastic stiffness of the mid-block specimens are, on average, greater than those of the corner specimens by 6.3% and 3.8%, respectively. These differences, and the associated data variability, were verified to be statistically insignificant and characteristic of a homogeneous CSEB material.
4) The uniaxial compressive strength and elastic stiffness of the specimens loaded perpendicularly to the compaction direction are, on average, greater than those of the specimens loaded in the compaction direction by up to 11.5% and 16.0%, respectively. These differences, and the associated data variability, were verified to be statistically insignificant and characteristic of an isotropic CSEB material.
5) From a practical standpoint, the manufacturing of homogeneous and isotropic CSEBs was not hindered by the physical heterogeneity of the soil mixture, the variability of its properties (*e.g.*, sand, silt and clay contents, particle size distribution, Atterberg limits), and relevant mechanisms associated with CSEB compaction and soil stabilization (*e.g.*, friction between soil mixture and mold surfaces, formation and distribution of cement hydrates).
6) A single probability distribution may be used to describe the variability of uniaxial compressive strength as well as elastic stiffness. The normal distribution may be more suitable for applications focused on the body of the distribution whereas the truncated normal distribution may be more suitable for applications focused on the distribution tails.

## DATA AVAILABILITY STATEMENT

All data used during the study are available in a repository in accordance with funder data retention policies. Repository: NSF NHERI DesignSafe; project number: PRJ-2809; project title: Physico-Mechanical Characterization of Homogeneity and Isotropy of Prototype Earth Block Material. DOIs: 10.17603/ds2-c6ta-x942 (soil characterization), 10.17603/ds2-fwxr-4373 (SEM and EDS analysis), and 10.17603/ds2-9ph0-vd80 (uniaxial compression tests). All data that support the findings of this study are also available from the corresponding author upon reasonable request.

## ACKNOWLEDGMENTS

The authors gratefully acknowledge the following support: National Science Foundation (NSF) through collaborative research awards #1537776 (University of South Carolina), #1537078 (Louisiana State University), and 1850777 (University of California, Davis); Electric Power Research Institute (EPRI) through award #DKT200194; University of South Carolina Office of the Vice President for Research, ASPIRE-I Program, through award #15520-14-35834; and, University of California Office of the President, Laboratory Fees Research Program, through award #LFR-20-651032. Special thanks are extended to: Richardson Construction Company (Columbia, SC) for supplying the soil; and NSF REU assistants Ms. Addison Darr, Mr. Christopher Frishcosy, and Mr. Hunter Jones.

## CREDIT AUTHOR STATEMENT

**Erika Rengifo-López**: Methodology, Validation, Formal Analysis, Investigation, Data Curation, Writing - Original Draft, Writing - Review & Editing, Visualization. **Nitin Kumar**: Methodology, Validation, Formal Analysis, Investigation, Data Curation, Writing - Original Draft, Writing - Review & Editing, Visualization. **Fabio Matta**: Conceptualization, Methodology, Validation, Formal Analysis, Data Curation, Writing - Original Draft, Writing - Review & Editing, Visualization, Supervision, Project Administration, Funding Acquisition. **Michele Barbato**: Conceptualization, Methodology, Validation, Formal Analysis, Data Curation, Writing - Original Draft, Writing - Review & Editing, Supervision, Project Administration, Funding Acquisition.

## NOTATION

*The following symbols are used in this paper:*

AD = Anderson-Darling.

C = Designation for CSEB cube specimen extracted from block corner location.

CDF = cumulative distribution function.

CV = coefficient of variation.

$f_{\mathrm{CSEB}}$ = average compression stress of CSEB cube specimen at failure.

IQR = interquartile range.

$K_{\mathrm{CSEB}}$ = elastic stiffness of CSEB cube specimen along compression load direction.

SD = standard deviation.

M = Designation for CSEB cube specimen extracted from mid-block location.

X = Designation for CSEB cube specimen loaded along X axis.

Y = Designation for CSEB cube specimen loaded along Y axis.

Z = Designation for CSEB cube specimen loaded along Z axis (compaction direction).

# REFERENCES

ASCE. 2000. *Prestandard and commentary for the seismic rehabilitation of buildings*. FEMA 356. Washington, DC: ASCE.

ASTM. 2012. *Standard test methods for laboratory compaction characteristics of soil using standard effort (12,400 ft-lbf/ft$^3$ (600 kN-m/m$^3$))*. ASTM D698-12. West Conshohocken, PA: ASTM.

ASTM. 2016. *Standard guide for design of earthen wall building systems*. ASTM E2392-10. West Conshohocken, PA: ASTM.

ASTM. 2017a. *Standard practice for classification of soils for engineering purposes (Unified Soil Classification System)*. ASTM D2487-17. West Conshohocken, PA: ASTM.

ASTM. 2017b. *Standard test methods for liquid limit, plastic limit, and plasticity index of soils*. ASTM D4318-17. West Conshohocken, PA: ASTM.

ASTM. 2017c. *Standard test method for particle-size distribution (gradation) of fine-grained soils using the sedimentation (hydrometer) analysis*. ASTM D7928-17. West Conshohocken, PA: ASTM.

ASTM. 2017d. *Standard test method for particle-size distribution (gradation) of soils using sieve analysis*. ASTM D6913-17. West Conshohocken, PA: ASTM.

Aubert, J. E., P. Maillard, J. C. Morel, and M. Al Rafii. 2016. “Towards a simple compressive strength test for earth bricks?” *Mater. Struct.*, 49 (5): 1641–1654. https://doi.org/10.1617/s11527-015-0601-y.

Bui, Q.-B., and J.-C. Morel. 2009. “Assessing the anisotropy of rammed earth.” *Constr. Build. Mater.*, 23 (9): 3005–3011. https://doi.org/10.1016/j.conbuildmat.2009.04.011.

Bui, Q.-B., J.-C. Morel, S. Hans, and N. Meunier. 2009. “Compression behavior of non-industrial materials in civil engineering by three scale experiments: the case of rammed earth.” *Mater. Struct.*, 42 (8): 1101–1116. https://doi.org/10.1617/s11527-008-9446-y.

Cabané, A., L. Pelà, and P. Roca. 2022. “Anisotropy and compressive strength evaluation of solid fired clay bricks by testing small specimens.” *Constr. Build. Mater.*, 344: 128195, 12 p. https://doi.org/10.1016/j.conbuildmat.2022.128195.

Ciancio, D., and J. Gibbings. 2012. “Experimental investigation on the compressive strength of cored and molded cement-stabilized rammed earth samples.” *Constr. Build. Mater.*, 28 (1): 294–304. https://doi.org/10.1016/j.conbuildmat.2011.08.070.

Cuéllar-Azcárate, M. C. 2016. “Engineered earthen masonry structures for extreme wind loads.” PhD dissertation. Columbia, SC: University of South Carolina.

D'Agostino, R. B., and M. A. Stephens. 1986. *Goodness-of-fit Techniques*. Boca Raton, FL: CRC Press.

Erdogmus, E., B. Skourup, E. Garcia, and F. Matta. 2019. "Tornado resistant residential design using experimentally obtained characteristic values for cement stabilized earthen masonry," *J. Archit. Eng.*, 25(2), 04019012. https://doi.org/10.1061/(ASCE)AE.1943-5568.0000342.

Gibbons, J. D., and S. Chakraborti. 2020. *Nonparametric statistical inference*. Boca Raton, FL: CRC press.

Glass, G. V. 1966. "Testing homogeneity of variances." *Am. Educ. Res. J.*, 3 (3): 187–190. Sage Publications.

Glass, G. V., P. D. Peckham, and J. R. Sanders. 1972. "Consequences of failure to meet assumptions underlying the fixed effects analyses of variance and covariance." *Rev. Educ. Res.*, 42 (3): 237–288. https://doi.org/10.3102/00346543042003237.

González-López, J. R., C. A. Juárez-Alvarado, B. Ayub-Francis, and J. M. Mendoza-Rangel. 2018. "Compaction effect on the compressive strength and durability of stabilized earth blocks." *Constr. Build. Mater.*, 163: 179–188. https://doi.org/10.1016/j.conbuildmat.2017.12.074.

Gooding, D. E. M. 1993. "Quasi-static compression forming of stabilised soil-cement building blocks." Working Paper No. 40. Coventry, UK: Development Technology Unit, Department of Engineering, University of Warwick.

Gooding, D. E. M. 1994. "Improved processes for the production of soil-cement building blocks." PhD dissertation. Coventry, UK: University of Warwick.

Harding, B., C. Tremblay, and D. Cousineau. 2014. "Standard errors: A review and evaluation of standard error estimators using Monte Carlo simulations." *Quant. Methods Psychol.*, 10 (2): 107–123.

Hollander, M., D. A. Wolfe, and E. Chicken. 2015. *Nonparametric statistical methods*. 3rd ed. Hoboke, NJ: John Wiley & Sons.

ICC (International Code Council). 2021. *International building code*. Section 2109 "Empirical design of adobe masonry." Washington, DC: ICC.

Illampas, R., I. Ioannou, and D. Charmpis. 2014. "Adobe bricks under compression: Experimental investigation and derivation of stress–strain equation." *Constr. Build. Mater.*, 53: 83–90. https://doi.org/10.1016/j.conbuildmat.2013.11.103.

Islam, M. S., T. E. Elahi, A. R. Shahriar, K. Nahar, and T. R. Hossain. 2020. "Strength and durability characteristics of cement-sand stabilized earth blocks." *J. Mater. Civ. Eng.*, 32 (5): 04020087, 15 p. https://doi.org/10.1061/(ASCE)MT.1943-5533.0003176.

Jiménez Delgado, M. C., and I. Cañas Guerrero. 2007. "The selection of soils for unstabilised earth building: A normative review." *Constr. Build. Mater.*, 21 (2): 237–251. https://doi.org/10.1016/j.conbuildmat.2005.08.006.

Kececioglu, D. 2002. *Reliability & life testing handbook*. Lancaster, PA: DEStech Publications, Inc.

Kumar, N., M. Barbato, and R. Holton. 2018. "Feasibility study of affordable earth masonry housing in the US Gulf Coast." *J. Archit. Eng.*, 24 (2): 04018009. https://doi.org/10.1061/(ASCE)AE.1943-5568.0000311.

Kumar, N., M. Barbato, E.L. Rengifo-López, and F. Matta. 2022. "Capabilities and limitations of existing finite element simplified micro-modeling techniques for unreinforced masonry." *Res. Eng. Struct. Mat.*, 8(3), 463–490. http://dx.doi.org/10.17515/resm2022.408st0226.

Kumar, N., M. Barbato, E.L. Rengifo-López, and F. Matta. 2023. "Finite element detailed micromodeling of unreinforced earth block masonry," *J. Struct. Eng.*, 149 (7), 04023081, 14 p. https://doi.org/10.1061/JSENDH.STENG-12093.

Levene, H. 1960. "Robust tests for equality of variances." *Contributions to probability and statistics: essays in honor of Harold Hotelling*, 278–292. Palo Alto, CA: Stanford University Press.

Lix, L. M., J. C. Keselman, and H. J. Keselman. 1996. "Consequences of assumption violations revisited: a quantitative review of alternatives to the one-way analysis of variance *F*-test." *Rev. Educ. Res.*, 66 (4): 579–619. https://doi.org/10.3102/00346543066004579.

Matta, F., M. C. Cuéllar-Azcárate, and E. Garbin. 2015. "Earthen masonry dwelling structures for extreme wind loads." *Eng. Struct.*, 83: 163–175. https://doi.org/10.1016/j.engstruct.2014.10.043.

McGill, R., J. W. Tukey, and W. A. Larsen. 1978. "Variations of box plots." *Am. Stat.*, 32 (1): 12–16. https://doi.org/10.1080/00031305.1978.10479236.

Miccoli, L., A. Garofano, P. Fontana, and U. Müller. 2015. "Experimental testing and finite element modelling of earth block masonry." *Eng. Struct.*, 104: 80–94. https://doi.org/10.1016/j.engstruct.2015.09.020.

Montgomery, D. C., G. C. Runger, and N. F. Hubele. 2009. *Engineering statistics*. John Wiley & Sons.

Morris, H. W., R. Walker, and T. Drupsteen. 2011. "Modern and historic earth buildings: Observations of the 4th September 2010 Darfield earthquake." In *Proc. 9th Pacific Conference on Earthquake Engineering (PCEE 2011)*, Paper No. 133. Auckland, New Zealand: New Zealand Society for Earthquake Engineering.

Morton, T. 2008. *Earth masonry design and construction guidelines*. Bracknell, UK: IHS BRE Press.

NM CPR (New Mexico State Commission of Public Records). 2016. *2015 New Mexico earthen building materials code.* NM Administrative Code (NMAC), Title 14, Chapter 7, Part 4. Santa Fe, NM: NM CPR.

Newbury, D. E., and N. W. M. Ritchie. 2013. "Is scanning electron microscopy/energy dispersive X-ray spectrometry (SEM/EDS) quantitative?" *Scanning*, 35 (3): 141–168. https://doi.org/10.1002/sca.21041.

Oliveira, O. M. de. 2004. "Estudo sobre a resistência ao cisalhamento de um solo residual compactado não saturado." PhD dissertation. São Paulo, Brasil: Universidade de São Paulo.

Piattoni, Q., E. Quagliarini, and S. Lenci. 2011. "Experimental analysis and modelling of the mechanical behaviour of earthen bricks." *Constr. Build. Mater.*, 25 (4): 2067–2075. https://doi.org/10.1016/j.conbuildmat.2010.11.039.

Rengifo-López, E. L. 2022. "Physico-mechanical characterization of prototype earth block material for constitutive modeling." PhD dissertation. Columbia, SC: University of South Carolina.

Rengifo-López, E. L., N. Kumar, F. Matta, and M. Barbato. 2017. "Variability of Compressive Strength and Stiffness of Compressed and Stabilized Earth Blocks." In *Proc. 9th International Earthbuilding Conference (Earth USA 2017)*, 242–247. Santa Fe, NM: Adobe in Action.

Rengifo-López, E. L., N. Kumar, F. Matta, and M. Barbato. 2018. "Can Compressed and Stabilized Earth Block Materials be Regarded as Homogeneous and Isotropic?" In *Proc. 10th International Masonry Conference (IMC 2018)*, 618–627. Whyteleafe, UK: International Masonry Society.

Rigassi, V. 1985. *Compressed earth blocks: Manual of production*. Eschborn, Germany: Deutsches Zentrum für Entwicklungstechnologien (GATE).

Ruiz, G., X. Zhang, W. F. Edris, I. Cañas, and L. Garijo. 2018. "A comprehensive study of mechanical properties of compressed earth blocks." *Constr. Build. Mater.*, 176: 566–572. https://doi.org/10.1016/j.conbuildmat.2018.05.077.

Rutherford, A. 2011. *ANOVA and ANCOVA: a GLM approach*. Hoboken, NJ: Wiley.

Silveira, D., H. Varum, and A. Costa. 2013. "Influence of the testing procedures in the mechanical characterization of adobe bricks." *Constr. Build. Mater.*, 40: 719–728. https://doi.org/10.1016/j.conbuildmat.2012.11.058.

Sloane, R. L., and T. R. Kell. 1966. "The fabric of mechanically compacted kaolin." *Proc. 14th National. Conference on Clays and Clay Minerals*, S. W. Bailey, ed., 289–296. Berkeley, CA: Pergamon Press. https://doi.org/10.1016/B978-0-08-011908-3.50027-X.

Snedecor, G. W., and W. G. Cochran. 1989. *Statistical methods*. Ames, IA: Iowa State University Press.

Stephens, M. A. 1974. "EDF Statistics for goodness of fit and some comparisons." *J. Am. Stat. Assoc.*, 69 (347): 730–737. https://doi.org/10.2307/2286009.

Stephens, M. A. 1986. "Tests based on EDF statistics." *Goodness-of-fit techniques*, 97–193. Boca Raton, FL: CRC Press.

Streiner, D. L. 1996. "Maintaining standards: differences between the standard deviation and standard error, and when to use each." *Can. J. Psychiatry*, 41 (8): 498–502. https://doi.org/10.1177/070674379604100805.

Van Damme, H., and H. Houben. 2018. "Earth concrete. Stabilization revisited." *Cem. Concr. Res.*, 114: 90–102. https://doi.org/10.1016/j.cemconres.2017.02.035.

Venkatarama Reddy, B. V., and K. S. Jagadish. 2003. "Embodied energy of common and alternative building materials and technologies." *Energy Build.*, 35 (2): 129–137. https://doi.org/10.1016/S0378-7788(01)00141-4.

Vilane, B.R.T. 2010. "Assessment of stabilisation of adobes by confined compression tests." *Biosyst. Eng.*, 106 (4): 551–558. https://doi.org/10.1016/j.biosystemseng.2010.06.008.

Walker, P. J. 2004. "Strength and erosion characteristics of earth blocks and earth block masonry." *J. Mater. Civ. Eng.*, 16 (5): 497–506. https://doi.org/10.1061/(ASCE)0899-1561(2004)16:5(497).

Walker, P., and T. Stace. 1997. "Properties of some cement stabilised compressed earth blocks and mortars." *Mater. Struct.*, 30 (9): 545–551. https://doi.org/10.1007/BF02486398.

# TABLES

**Table 1.** Salient results of soil characterization.

| **Property** | **Range [%]** |
|---|---|
| Sand content (passing No.4 sieve, retained on No. 200 sieve) | 53.6±0.95 |
| Silt content (particle size in range 0.074–0.005 mm) | 15.1±1.47 |
| Clay content (particle size < 0.005 mm) | 31.4±1.47 |
| Liquid limit | 39.1±3.26 |
| Plastic limit | 20.3±2.21 |
| Plasticity index | 18.9±1.95 |
| Optimum moisture content | 14.3±1.48 |

**Table 2.** Test matrix for characterization of uniaxial compressive response of CSEB material.

| **Load direction** | **Specimen location (in source CSEB)** | | **Number of specimens (by load direction)** |
|---|---|---|---|
| | **Corner (C)** | **Mid-block (M)** | |
| X | 18 | 10 | 28 |
| Y | 18 | 10 | 28 |
| Z | 20 | 8 | 28 |
| **Number of specimens (by location)** | 56 | 28 | Total = 84 |

**Table 3.** Uniaxial compressive strength ($f_{CSEB}$) results for CSEB specimens [MPa].

| Source CSEB | Specimen location (C, M) and load direction (X, Y, Z) | | | | | | | | | Mean | CV [%] |
|---|---|---|---|---|---|---|---|---|---|---|---|
| | X | | | Y | | | Z | | | | |
| | C | | M | C | | M | C | | M | | |
| B01 | 4.48 | | 4.14 | 4.07 | | 5.08 | 3.91 | 3.66 | - | 4.22 | 11.8 |
| B02 | 4.79 | 4.62 | - | 4.39 | | 4.51 | 5.49 | | 4.38 | 4.70 | 8.9 |
| B03 | 3.31 | | 3.28 | 3.03 | | 3.63 | 2.69 | 3.66 | - | 3.27 | 11.3 |
| B04 | 4.12 | | 4.65 | 3.86 | 3.70 | - | 3.75 | | 3.49 | 3.93 | 10.5 |
| B05 | 2.92 | | 2.73 | 3.03 | | 2.63 | 2.24 | 2.83 | - | 2.73 | 10.1 |
| B06 | 2.41 | | 2.38 | 2.30 | | 2.15 | 1.89 | 1.87 | - | 2.17 | 11.1 |
| B07 | 1.29 | | 2.11 | | | - | 1.41 | | 1.80 | 1.64 | 18.5 |
| B08 | 2.26 | 3.08 | - | 3.20 | | 3.51 | 2.81 | | 2.93 | 2.96 | 14.3 |
| B09 | 4.31 | 4.00 | - | 3.37 | | 3.34 | 2.85 | | 3.79 | 3.61 | 14.6 |
| B10 | 3.26 | | 4.73 | 4.38 | | 4.31 | 3.51 | 3.86 | - | 4.01 | 14.0 |
| B11 | 2.38 | 2.44 | - | 2.49 | | 2.66 | 2.50 | | 1.93 | 2.40 | 10.3 |
| B12 | 4.61 | | 4.35 | 4.36 | 4.25 | - | 2.64 | | 5.42 | 4.27 | 21.2 |
| B13 | 4.92 | | 3.50 | 4.03 | | 3.98 | 2.53 | 4.47 | - | 3.91 | 21.1 |
| B14 | 4.74 | | 4.04 | 3.62 | 4.34 | - | 2.57 | | 3.63 | 3.83 | 19.6 |

**Table 4.** Mean and CV of uniaxial compressive strength ($f_{CSEB}$) for significant groups of CSEB specimens.

| Specimen group | All | By location | | By load direction | | |
|---|---|---|---|---|---|---|
| | | C | M | X | Y | Z |
| **Number of specimens** | 84 | 56 | 28 | 28 | 28 | 28 |
| **Mean [MPa]** | 3.40 | 3.33 | 3.54 | 3.57 | 3.48 | 3.16 |
| **CV [%]** | 29.3 | 30.2 | 27.7 | 28.8 | 26.1 | 32.8 |

**Table 5.** Elastic stiffness ($K_{CSEB}$) results for CSEB specimens [kN/mm].

| Source CSEB | Specimen location (C, M) and load direction (X, Y, Z) | | | | | | | | | Mean | CV [%] |
|---|---|---|---|---|---|---|---|---|---|---|---|
| | X | | | Y | | | Z | | | | |
| | C | | M | C | | M | C | | M | | |
| B01 | 15.6 | | 19.2 | 22.7 | | 22.1 | 15.1 | 16.8 | - | 18.6 | 17.7 |
| B02 | 21.9 | 18.4 | - | 15.0 | | 19.6 | 16.0 | | 20.0 | 18.5 | 14.0 |
| B03 | 10.6 | | N/A | 10.9 | | 12.8 | 8.04 | 9.55 | - | 10.4 | 17.1 |
| B04 | 15.0 | | 14.3 | 12.3 | 12.5 | - | | | 12.4 | 13.0 | 10.1 |
| B05 | 9.55 | | 8.46 | 9.81 | | 8.43 | 10.6 | 7.76 | - | 9.10 | 11.5 |
| B06 | 9.46 | | 7.06 | 7.88 | | 7.98 | 6.69 | 5.83 | - | 7.48 | 16.7 |
| B07 | 6.57 | | 6.79 | 5.61 | 5.46 | | 6.17 | | 5.34 | 5.99 | 10.1 |
| B08 | 6.07 | 10.2 | - | 10.1 | | 12.0 | 7.91 | | 8.61 | 9.14 | 22.7 |
| B09 | 18.0 | 16.1 | - | 13.8 | | 13.4 | 13.1 | | 17.5 | 15.3 | 14.3 |
| B10 | 15.1 | | 19.0 | 15.4 | | 14.2 | 14.8 | 16.0 | - | 15.8 | 10.8 |
| B11 | 10.5 | 11.9 | - | 11.9 | | 9.83 | 8.72 | | 7.71 | 10.1 | 16.8 |
| B12 | 21.7 | | 16.1 | 17.8 | 18.0 | - | 10.8 | | 21.1 | 17.6 | 22.5 |
| B13 | 21.3 | | 15.7 | 15.9 | | 14.6 | 12.3 | 20.8 | - | 16.8 | 21.2 |
| B14 | 22.5 | | 21.0 | 16.7 | 18.5 | - | 16.2 | | 12.5 | 17.9 | 20.2 |

**Table 6.** Mean and CV of elastic stiffness ($K_{CSEB}$) for significant groups of CSEB specimens.

| Specimen group | All | By location | | By load direction | | |
|---|---|---|---|---|---|---|
| | | C | M | X | Y | Z |
| **Number of specimens** | 83 | 56 | 27 | 27 | 28 | 28 |
| **Mean [kN/mm]** | 13.3 | 13.1 | 13.6 | 14.4 | 13.4 | 12.1 |
| **CV [%]** | 36.6 | 36.5 | 37.3 | 36.8 | 33.8 | 38.6 |

**Table 7.** *p*-values from Wilconox rank-sum test on $f_{CSEB}$ data.

| Specimen group | By location | | By load direction | | |
|---|---|---|---|---|---|
| | C | M | X | Y | Z |
| **All** | 0.99 | 0.65 | 0.40 | 0.73 | 0.23 |
| **C** | - | 0.63 | 0.43 | 0.77 | 0.30 |
| **M** | - | | 0.82 | 0.95 | 0.21 |
| **X** | - | | | 0.62 | 0.12 |
| **Y** | - | | | | 0.18 |

**Table 8.** *p*-values from Wilconox rank-sum test on $K_{CSEB}$ data.

| Specimen group | By location | | By load direction | | |
|---|---|---|---|---|---|
| | C | M | X | Y | Z |
| **All** | 0.86 | 0.79 | 0.35 | 0.90 | 0.29 |
| **C** | - | 0.96 | 0.47 | 0.99 | 0.26 |
| **M** | - | | 0.59 | 0.89 | 0.30 |
| **X** | - | | | 0.46 | 0.12 |
| **Y** | - | | | | 0.31 |

**Table 9.** CV of mean and SD of $f_{CSEB}$ for different specimen groups.

| Specimen group | Number of specimens | Mean [MPa] | SD [MPa] | Standard error [MPa] | | CV [%] | |
|---|---|---|---|---|---|---|---|
| | | | | Mean | SD | Mean | SD |
| All | 84 | 3.40 | 1.00 | 0.109 | 0.077 | 3.2 | 7.7 |
| C | 56 | 3.33 | 0.97 | 0.129 | 0.092 | 3.9 | 9.5 |
| M | 28 | 3.54 | 1.05 | 0.199 | 0.144 | 5.6 | 13.7 |
| X | 28 | 3.57 | 1.03 | 0.194 | 0.140 | 5.5 | 13.6 |
| Y | 84 | 3.40 | 1.00 | 0.109 | 0.077 | 3.2 | 7.7 |
| Z | 56 | 3.33 | 0.97 | 0.129 | 0.092 | 3.9 | 9.5 |

**Table 10.** CV of mean and SD of $K_{CSEB}$ for different specimen groups.

| Specimen group | Number of specimens | Mean [kN/mm] | SD [kN/mm] | Standard error [kN/mm] | | CV [%] | |
|---|---|---|---|---|---|---|---|
| | | | | Mean | SD | Mean | SD |
| All | 84 | 13.30 | 4.87 | 0.531 | 0.378 | 4.0 | 7.8 |
| C | 56 | 13.13 | 4.80 | 0.641 | 0.457 | 4.9 | 9.5 |
| M | 28 | 13.63 | 5.09 | 0.962 | 0.692 | 7.1 | 13.6 |
| X | 28 | 14.38 | 5.30 | 1.001 | 0.721 | 7.0 | 13.6 |
| Y | 28 | 13.40 | 4.52 | 0.855 | 0.615 | 6.4 | 13.6 |
| Z | 28 | 12.14 | 4.68 | 0.884 | 0.637 | 7.3 | 13.6 |

**Table 11.** *p*-values from two-sample *t*-test on $f_{CSEB}$ means.

| Specimen group | By location | | By load direction | | |
|---|---|---|---|---|---|
| | C | M | X | Y | Z |
| **All** | 0.87 | 0.53 | 0.46 | 0.72 | 0.28 |
| **C** | - | 0.49 | 0.42 | 0.65 | 0.38 |
| **M** | - | | 0.93 | 0.82 | 0.18 |
| **X** | - | | | 0.74 | 0.15 |
| **Y** | - | | | | 0.23 |

**Table 12.** *p*-values from two-sample *t*-test on $K_{CSEB}$ means.

| Specimen group | By location | | By load direction | | |
|---|---|---|---|---|---|
| | C | M | X | Y | Z |
| **All** | 0.81 | 0.76 | 0.33 | 0.92 | 0.27 |
| **C** | - | 0.91 | 0.46 | 0.93 | 0.24 |
| **M** | - | | 0.60 | 0.86 | 0.26 |
| **X** | - | | | 0.46 | 0.10 |
| **Y** | - | | | | 0.31 |

**Table 13.** *p*-values from two-sample *F*-test on $f_{CSEB}$ standard deviations.

| Specimen group | By location | | By load direction | | |
|---|---|---|---|---|---|
| | C | M | X | Y | Z |
| **All** | 0.78 | 0.68 | 0.80 | 0.60 | 0.76 |
| **C** | - | 0.85 | 0.97 | 0.48 | 0.93 |
| **M** | - | | 0.90 | 0.44 | 0.93 |
| **X** | - | | | 0.52 | 0.96 |
| **Y** | - | | | | 0.49 |

**Table 14.** *p*-values from two-sample *F*-test on $K_{CSEB}$ standard deviations.

| Specimen group | By location | | By load direction | | |
|---|---|---|---|---|---|
| | C | M | X | Y | Z |
| **All** | 0.73 | 0.74 | 0.55 | 0.68 | 0.84 |
| **C** | - | 0.95 | 0.76 | 0.53 | 0.66 |
| **M** | - | | 0.84 | 0.55 | 0.67 |
| **X** | - | | | 0.42 | 0.53 |
| **Y** | - | | | | 0.86 |

812 **Table 15.** *p*-values from AD test for different statistical distributions of $f_{CSEB}$ and $K_{CSEB}$.
813

| Mechanical parameter | Number of specimens | Statistical distribution | | |
|---|---|---|---|---|
| | | Normal | Log-normal | Truncated normal |
| $f_{CSEB}$ | 84 | 0.155 | 0.002 | 0.154 |
| $K_{CSEB}$ | 83 | 0.072 | 0.020 | 0.065 |

814

## LIST OF FIGURE CAPTIONS

**Fig. 1.** Local soil used to manufacture CSEB samples: (a) soil collection in Lexington, SC; (b) soil after crushing and sieving; and (c) soil particle size distribution.

**Fig. 2.** CSEB specimens for uniaxial compression tests: (a) block in hydraulic press; and (b) cubic specimens cut from single block after curing.

**Fig. 3.** Uniaxial compression test setup.

**Fig. 4.** Representative examples of CSEB material inhomogeneities in SEM micrographs with increasing magnification: (a) sand grains (in dashed circles) embedded in stabilized soil matrix; (b) close-up image of sand grain and voids introducing discontinuities in soil matrix; (c) typical micro-scale voids size and distribution; and (d) micro-scale flaky clay particles (in dashed ovals) with different sizes and orientations.

**Fig. 5.** Results of EDS analysis of seven CSEB sample areas, with magnification ranging from 100× to 5000×. For each chemical element, values indicate mean ± SD of mass percentage from all (seven) measurements.

**Fig. 6.** Representative microscopic images of random CSEB material samples at increasing magnification and associated two-dimensional Ca maps from EDS analysis: (a) 100×; (b) 500×; and (c) 5000×.

**Fig. 7.** Photographs of CSEB specimens showing typical columnar (vertical) cracks developed under uniaxial compression loads, indicating effectiveness of PTFE inserts: (a-b) during testing; and (c) after failure.

**Fig. 8.** Compressive load, stress, and axial displacement of 15 representative CSEB specimens based on location: (a) corner (C); and (b) mid-block (M). Bold lines indicate envelope for all C and M specimens, respectively.

**Fig. 9.** Compressive load, stress, and axial displacement of 15 representative CSEB specimens based on load direction: (a) X; (b) Y; and (c) Z (parallel to compaction direction). Bold lines indicate envelope for all X, Y and Z specimens, respectively.

**Fig. 10.** Notched box plot of compressive strength results for different groups (all specimens, by location, by load direction).

**Fig. 11.** Notched box plot of elastic stiffness results for different groups (all specimens, by location, by load direction).

**Fig. 12.** 95% confidence intervals of compressive strength for different groups (all specimens, by location, by load direction): (a) mean; and (b) standard deviation.

**Fig. 13.** 95% confidence intervals of elastic stiffness for different groups (all specimens, by location, by load direction): (a) mean; and (b) standard deviation.

## FIGURES

**(a)**

**(b)**

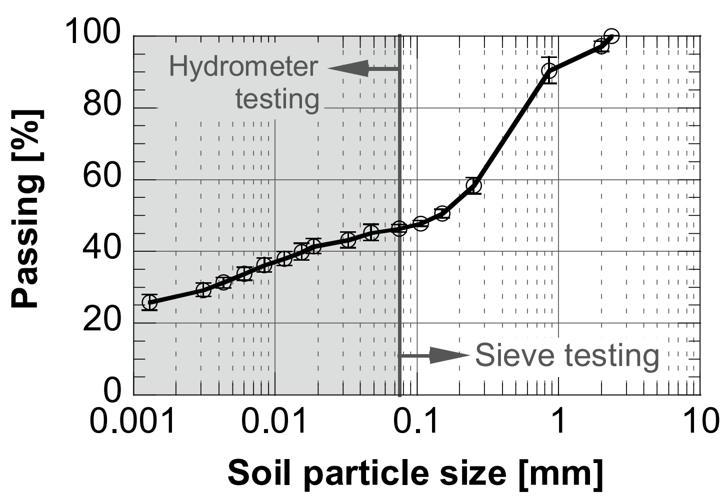


**(c)**

**Fig. 1.** Local soil used to manufacture CSEB samples: (a) soil collection in Lexington, SC; (b) soil after crushing and sieving; and (c) soil particle size distribution.


**(a)**

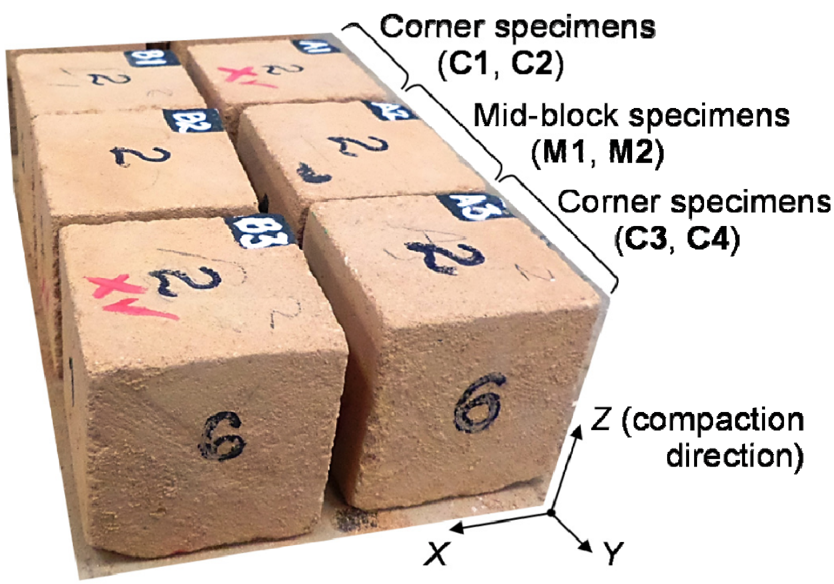


**(b)**

**Fig. 2.** CSEB specimens for uniaxial compression tests: (a) block in hydraulic press; and (b) cubic specimens cut from single block after curing.

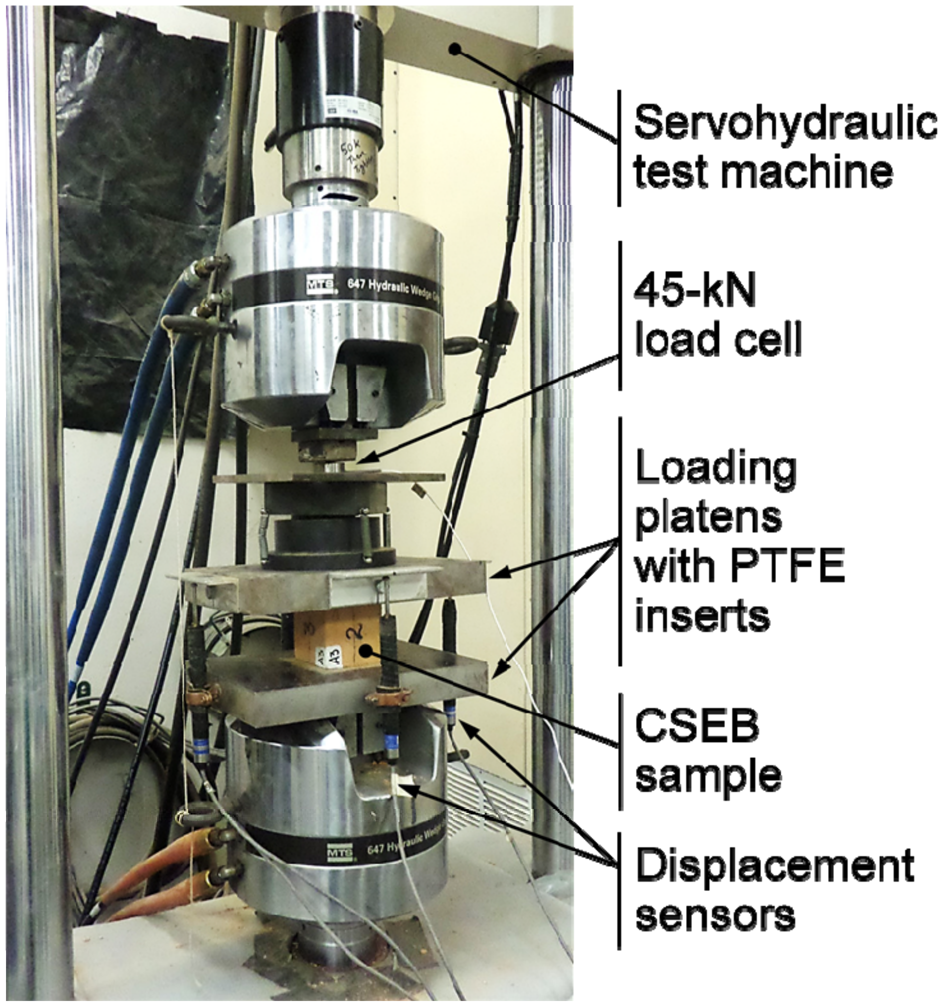


**Fig. 3.** Uniaxial compression test setup.

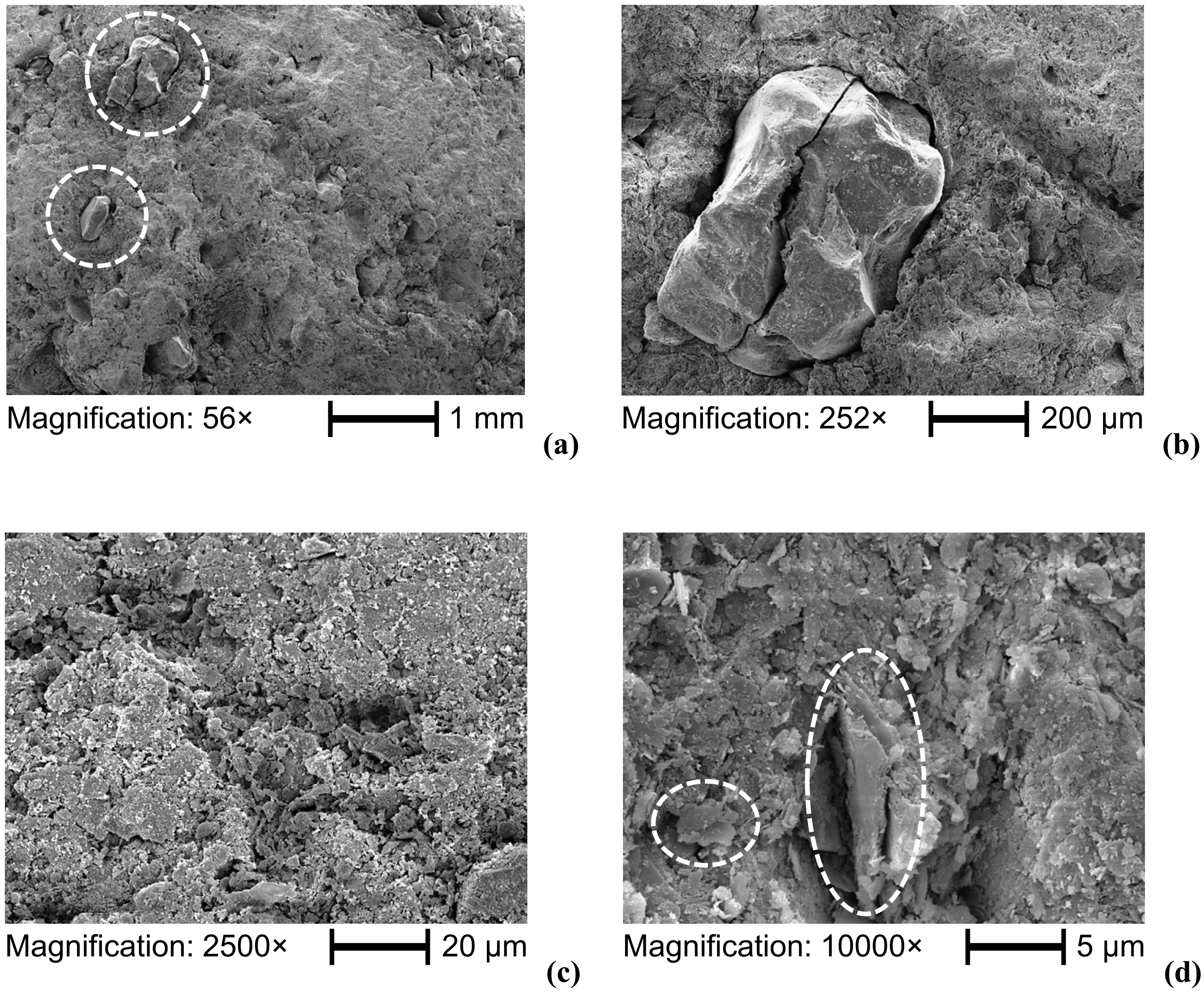


**Fig. 4.** Representative examples of CSEB material inhomogeneities in SEM micrographs with increasing magnification: (a) sand grains (in dashed circles) embedded in stabilized soil matrix; (b) close-up image of sand grain and voids introducing discontinuities in soil matrix; (c) typical micro-scale voids size and distribution; and (d) micro-scale flaky clay particles (in dashed ovals) with different sizes and orientations.

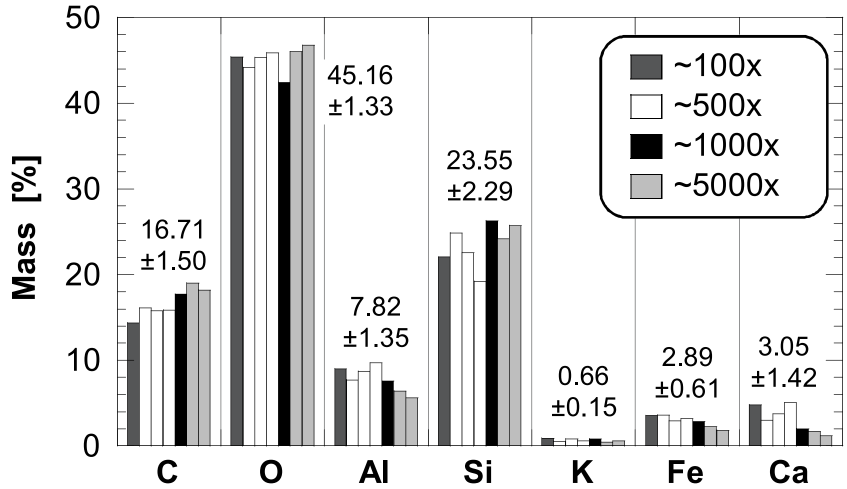


**Fig. 5.** Results of EDS analysis of seven CSEB sample areas, with magnification ranging from 100× to 5000×. For each chemical element, values indicate mean ± SD of mass percentage from all (seven) measurements.

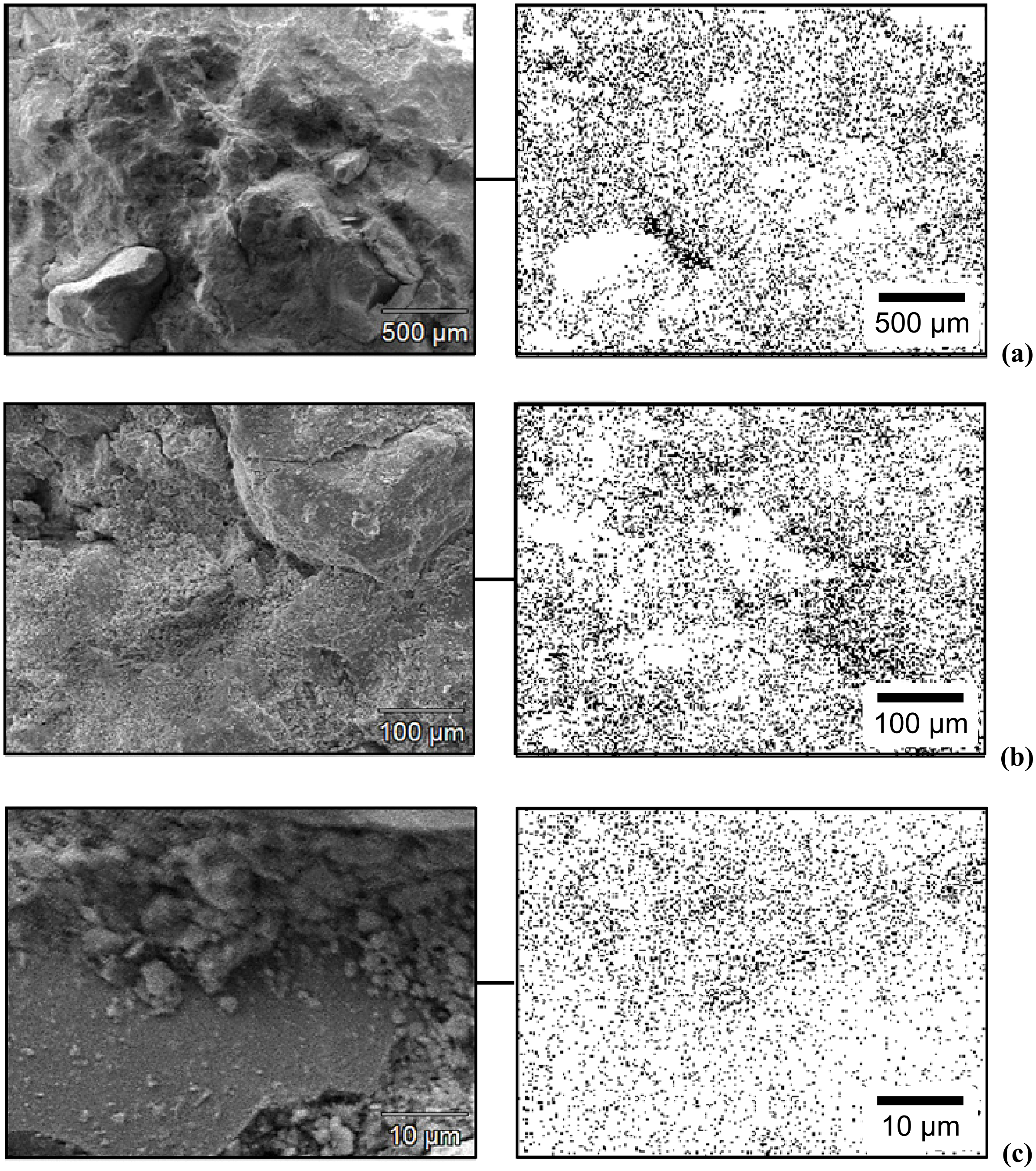


**Fig. 6.** Representative microscopic images of random CSEB material samples at increasing magnification and associated two-dimensional Ca maps from EDS analysis: (a) 100×; (b) 500×; and (c) 5000×.


**(a)**


**(b)**


**(c)**

**Fig. 7.** Photographs of CSEB specimens showing typical columnar (vertical) cracks developed under uniaxial compression loads, indicating effectiveness of PTFE inserts: (a-b) during testing; and (c) after failure.

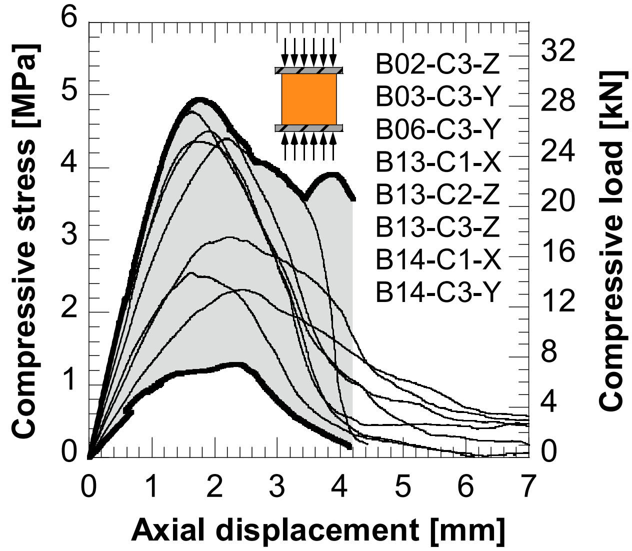


**(a)**

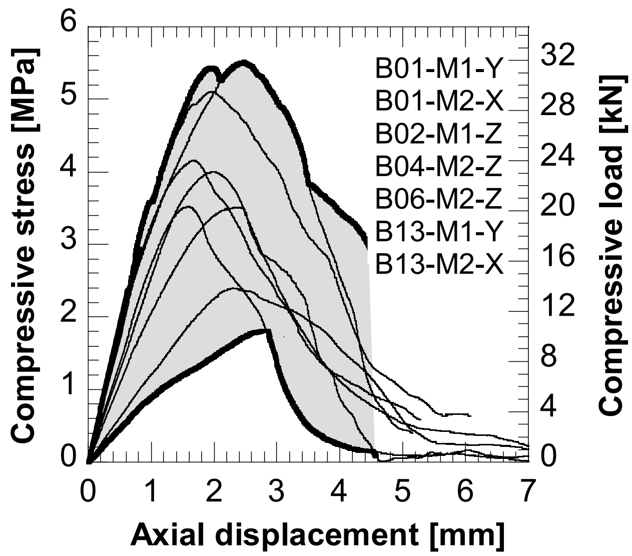


**(b)**

**Fig. 8.** Compressive load, stress, and axial displacement of 15 representative CSEB specimens based on location: (a) corner (C); and (b) mid-block (M). Bold lines indicate envelope for all C and M specimens, respectively.

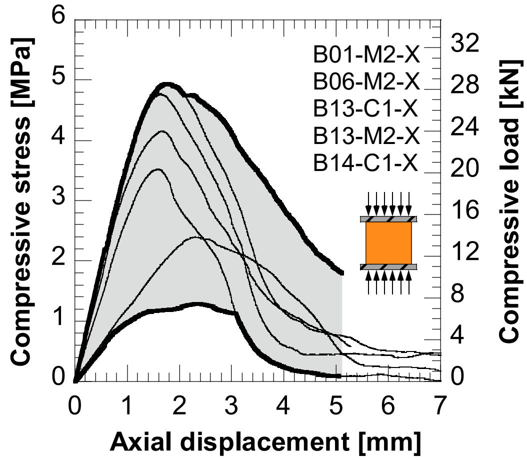


**(a)**

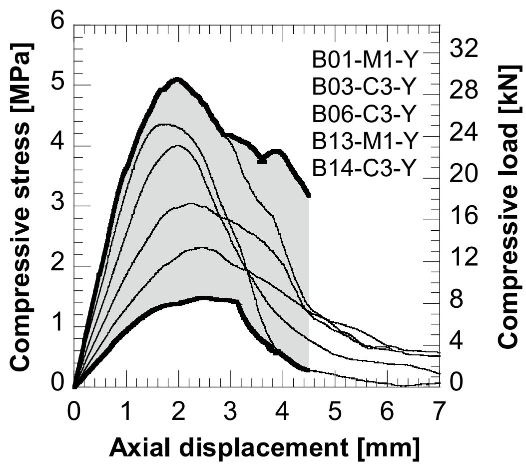


**(b)**

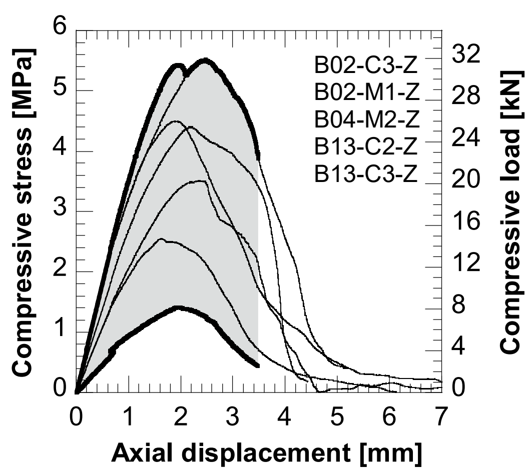


**(c)**

**Fig. 9.** Compressive load, stress, and axial displacement of 15 representative CSEB specimens based on load direction: (a) X; (b) Y; and (c) Z (parallel to compaction direction). Bold lines indicate envelope for all X, Y and Z specimens, respectively.

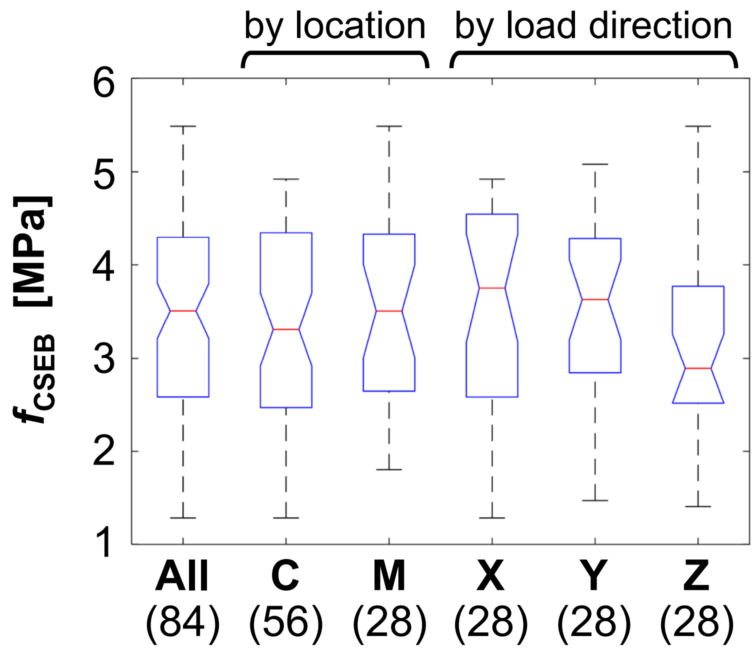


**Fig. 10.** Notched box plot of compressive strength results for different groups (all specimens, by location, by load direction).

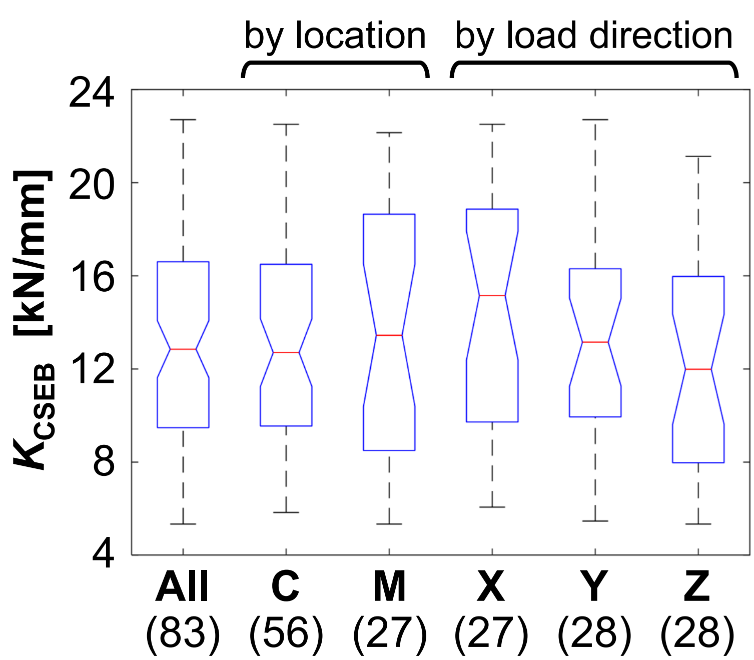


**Fig. 11.** Notched box plot of elastic stiffness results for different groups (all specimens, by location, by load direction).

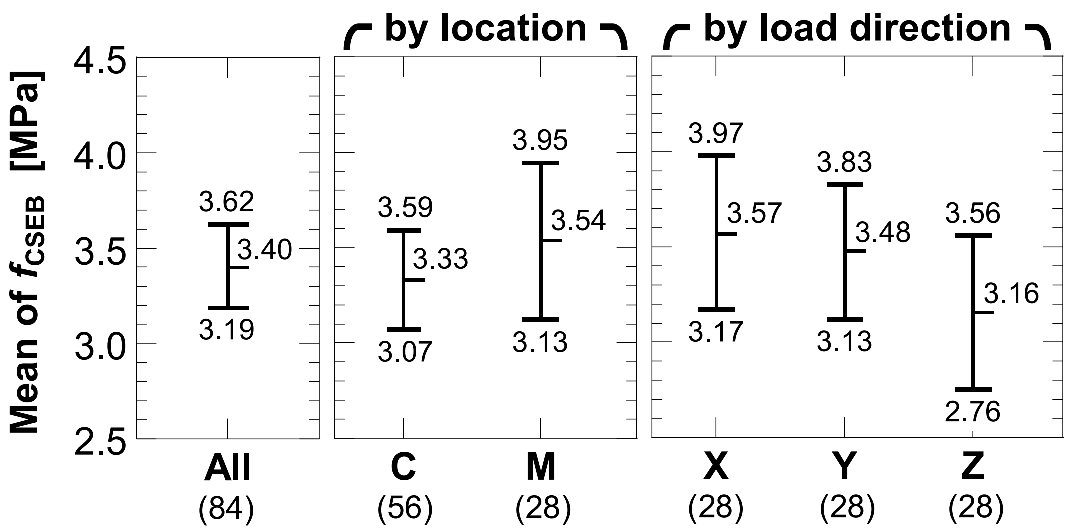


**(a)**

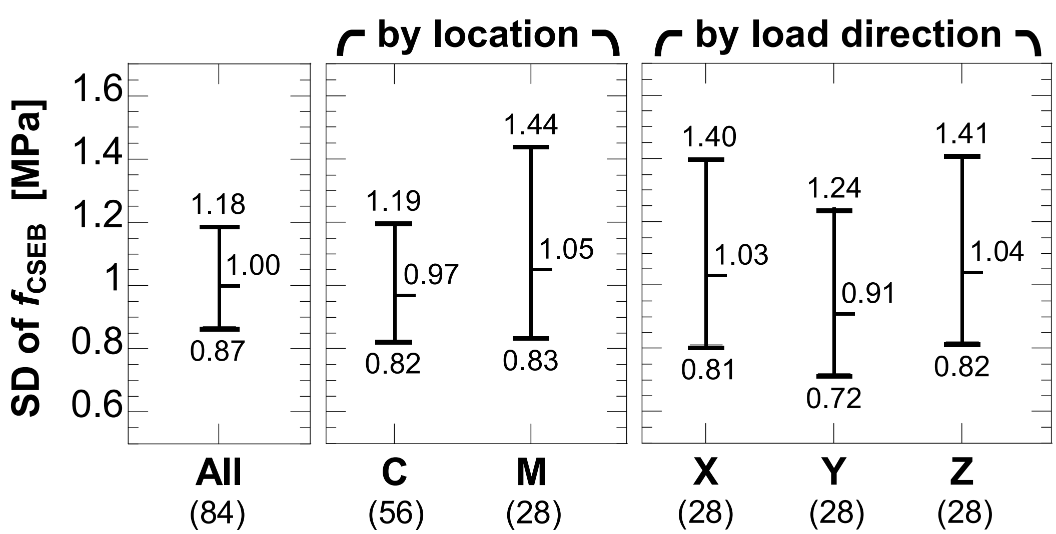


**(b)**

**Fig. 12.** 95% confidence intervals of compressive strength for different groups (all specimens, by location, by load direction): (a) mean; and (b) standard deviation.

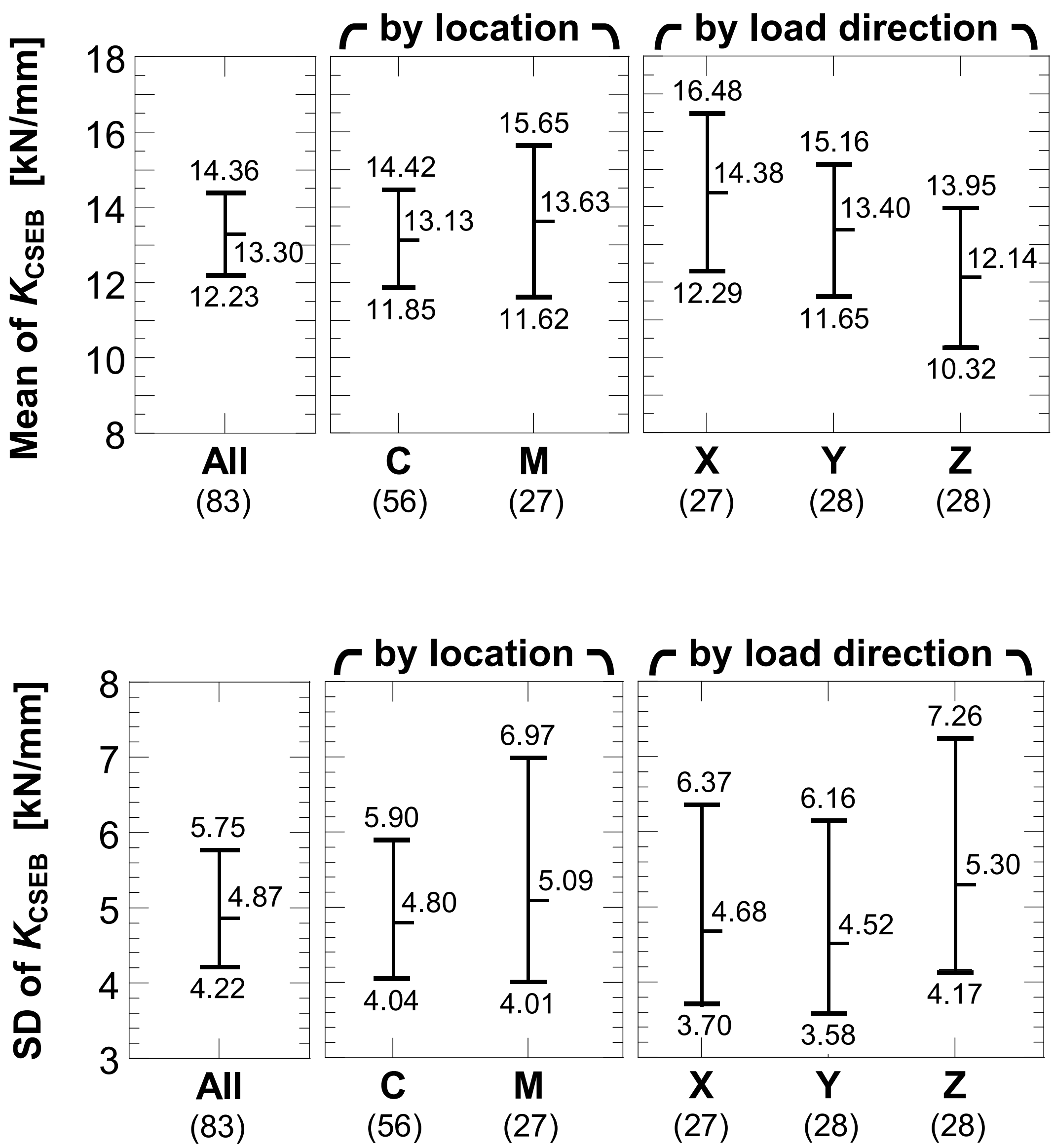


**(a)**

**(b)**

**Fig. 13.** 95% confidence intervals of elastic stiffness for different groups (all specimens, by location, by load direction): (a) mean; and (b) standard deviation.